Experimental Study on Shear Strength of Reinforced Concrete Beam-Column Joint with Different Anchorage Type for Beam Main Bar

Tianwen Dong [1*], *Nobuaki* Hanai[2], and *Toshiyuki* Kanakubo[1]

[1] University of Tsukuba, Tsukuba 305-8573, Japan
[2] Kyushu Sangyo Univ., Fukuoka 813-8503, Japan

Abstract. Experiments were conducted on reinforced concrete beam-column joints with different beam main bar anchorage types, and the shear strength of the joints was examined. In interior joints, the difference in beam main bar anchorage type resulted in lower joint shear strength for specimens with 90° bent anchorage compared to specimens with through beam bars. It could generally be evaluated using the shear strength calculation formula by the AIJ design guidelines using the anchorage length of the main bar. It considered that differences of the anchorage type of the beam main bar lead to the differences of the strut mechanism in the panel zone, resulting in different shear strength.

1 Introduction

In current design codes for reinforced concrete (RC) structures, the predicting formulas for the shear strength of beam–column joints are specified according to the joint configuration, such as interior or exterior joints, and the anchorage length of the beam main bars within the joint. However, little detailed discussion is provided for cases in which only the anchorage type of the beam main bars differs.

In most design codes (AIJ [1], ACI [2], Eurocode 8 [3], and NZS 3101 [4]), beam main bar is generally required to pass through the joint core in interior beam–column joints, as anchorage within the joint is considered unreliable due to severe bond deterioration and cracking under high shear stress. The intention of this requirement is not to assume perfect bond within the joint core, but rather to avoid relying on short anchorage in a region where bond deterioration and bar slip are difficult to prevent under cyclic loading, while ensuring stable force transfer through the confined joint core and preventing brittle joint or column failure. [5]

The precast RC frame systems have been widely used to improve construction efficiency and economy. In such systems, beam main bar is often anchored within the joint. For example, previous studies have investigated details in which the top bars were arranged as through-bars while the bottom bars were anchored using hooks [6]. Furthermore, if sufficient anchorage performance can be secured, it may also be possible to use hooked anchorage for both the top and bottom beam main bars.

In previous studies, the authors conducted reversed cyclic loading tests on interior RC beam–column joint specimens with two different beam main bar anchorage details, i.e., through-bars and hooked anchorage within the joint. [7] The experimental results showed that the maximum load of the specimens with hooked anchorage was more than 20% lower than that of conventional interior joints. In addition, it was observed that the internal stress transfer mechanism within the joint differed depending on the anchorage type.

To investigate these experimental findings more clearly and to observe the stress transfer mechanism within the joint, additional one-way static loading tests were conducted using similar specimens. Including the results of the previous experiments, the objective of this study is therefore to compare the shear strength of interior beam–column joint specimens with through-bar and hooked anchorage details.

2 Experimental Program

2.1 Test Specimens and Materials

Four RC beam–column joint specimens were fabricated and tested. The shapes, dimensions, and

* Corresponding author: s2536046@u.tsukuba.ac.jp

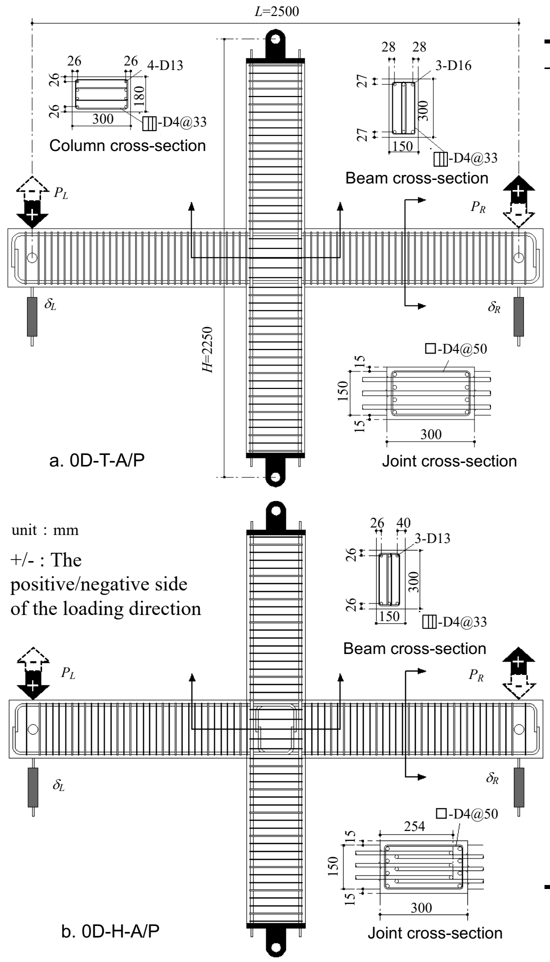

Fig. 1. Dimensions and reinforcement details of specimens

Table 1. List of specimens

			0D -T-A	0D -T-P	0D-H-A	0D-H-P
Specimen ID			0D -T-A	0D -T-P	0D-H-A	0D-H-P
Beam	Width ×Depth (mm)		150×300			
	Main bars		3-D16		3-D13	
		σ_y (MPa)	831	824	866	869
		E_s (GPa)	211	214	210	206
	Anchorage type		through bars		90-degree hooked bars	
	Stirrups		▥-D4@33, p_w=1.12%			
		σ_y (MPa)	399	379	399	372
		E_s (GPa)	191	195	191	196
Column	Width ×Depth (mm)		180×300			
	Main bars		8-D13			
		σ_y (MPa)	866	831	866	869
		E_s (GPa)	210	203	210	206
	Hoops		▥-D4@33, p_w=0.94%			
		in panel zone	□-D4@50, p_{jw}=0.31%			
		σ_y (MPa)	399	379	399	372
		E_s (GPa)	191	195	191	196
Loading history			Reversed cyclic	Oneway cyclic	Reversed cyclic	Oneway cyclic
Concrete		σ_B (MPa)	25.7	23.8	25.7	22.7
		σ_t (MPa)	2.38	2.39	2.38	2.69
		E_c (GPa)	25.4	24.7	25.4	24.3

where σ_y: yield strength E_s: Young's modulus

σ_B: compressive strength σ_t: tensile strength

E_c: Young's modulus

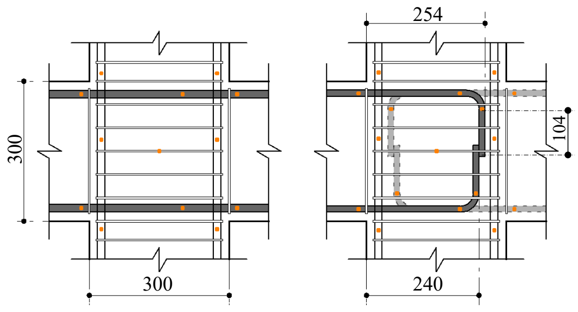

Fig. 2. Joint details of specimens

reinforcement details of the specimens are shown in Fig. 1. Table 1 shows the list of specimens. The targeted RC frame has a span of 2500 mm and a story height of 2250 mm, corresponding to about 1/3 scale model of an actual structure. To prevent failure of the beams and columns and to focus on the failure of the joint, high-strength reinforcing bars were used for the main bars, and sufficient stirrups and hoops were arranged.

The main variables of the specimens are the anchorage type of the main bars of the beam. In the T-series specimens, the beam main bars were arranged as through-bars passing through the joint, whereas in the H-series specimens, the beam main bars were anchored within the joint using standard hooks (90-degree bends). The detailed reinforcement arrangements of specimens are shown in Fig. 2.

2.2 Loading and Measurement

The column top and bottom were pin-supported, and a pair of actuators applied anti-symmetric displacements for beams at points located 1100 mm from each column face. Specimens 0D-T-A and 0D-H-A was subjected to fully reversed cyclic loading, while the remaining specimens were subjected to one-way cyclic loading, as each cycle was unloaded to zero before proceeding to the next cycle.

The drift angle was calculated as the sum of the left and right actuator displacements divided by the span length (2500 mm). The shear deformation of the joint was measured as shown in Fig.3. No axial load was applied to the column.

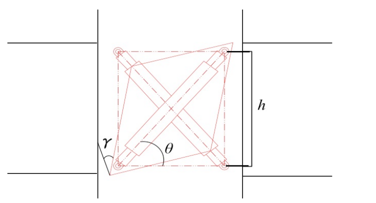

$\gamma=(\delta_1-\delta_2)/2h\cos\theta$
where,
γ: Shear deformation angle
δ_1, δ_2 : Diagonal deformation
h : Vertical length of the measured section

Fig. 3. Measurement of shear deformation in panel zone

3 Test Results

3.1 Applied Load–Drift Angle Response and Failure Mode

Fig.4 shows the applied load (P_{exp})–drift angle (R) relationships, where P_{exp} is the average load of the two beam actuators. The maximum applied loads are also shown in the figure. Fig.5 shows the shear force–shear deformation angle relationships of the joint. The shear force was calculated by Eq. (1).

$$V_{jexp} = \{(L-D_c)/j_b - L/H\}P_{exp} \qquad (1)$$

where,

L: span length
D_c: depth of column
j_b: distance between the compressive and tensile forces of beam (=7/8d)
d: effective depth of beam
H: story height
P_{exp}: applied load

Compared with the specimen employing hooked bar anchorage, the specimen with through-bars exhibited lower strength. The maximum load of specimens 0D-T-A, 0D-T-P and 0D-H-A were observed at 20 × 10-3 rad. Specimen 0D-H-P was observed at 25 × 10-3 rad. The maximum load of the 0D-H-A specimen was approximately 25% lower than that of the 0D-T-A specimen, while that of the 0D-H-P specimen was approximately 11% lower than that of the 0D-T-P specimen. Although specimen 0D-T-A showed a slightly higher positive peak load than specimen 0D-T-P, this difference should be interpreted with caution because the two specimens were subjected to different loading histories. Specimen 0D-T-A was tested under fully reversed cyclic loading, whereas specimen 0D-T-P was subjected to one-way cyclic loading. The slightly higher peak load observed in 0D-T-A may be attributed to changes in bond stress distribution and internal force redistribution caused by prior load reversals, which can temporarily enhance the apparent load-carrying capacity in one loading direction. However, 0D-T-A exhibited more rapid post-peak degradation under cyclic reversals, indicating greater damage accumulation in the joint. Therefore, the higher positive peak of 0D-T-A is not interpreted as an enhancement due to reversed loading, but rather as a consequence of loading-history-dependent behavior and experimental variability within a limited test series.

Fig.6 shows the crack patterns and failure progress. In the specimens with through-bars, typical diagonal shear cracks connecting the compression zones of the beam and column were observed. In contrast, the specimens with hooked bar anchorage exhibit-ed inclined cracks extending from the compression zones

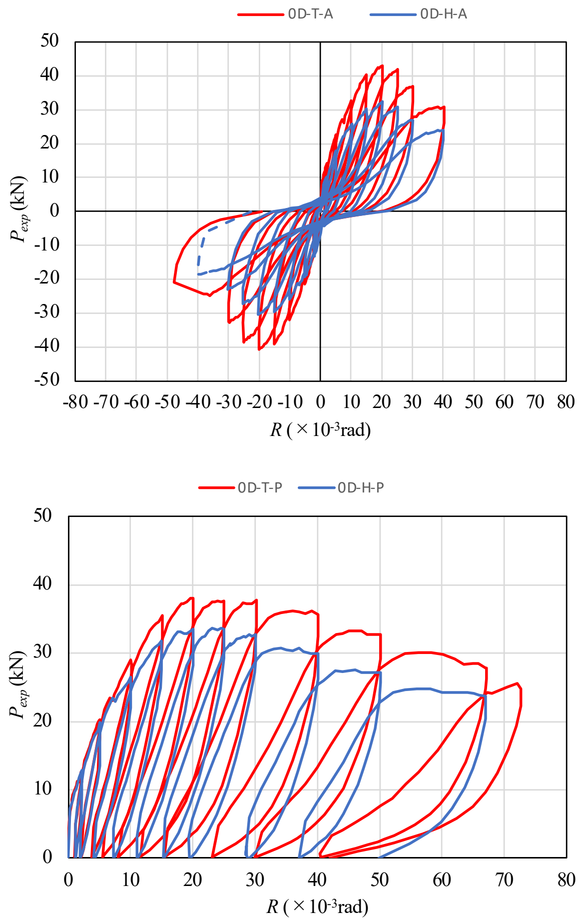

Fig. 4. Applied load–drift angle relationship

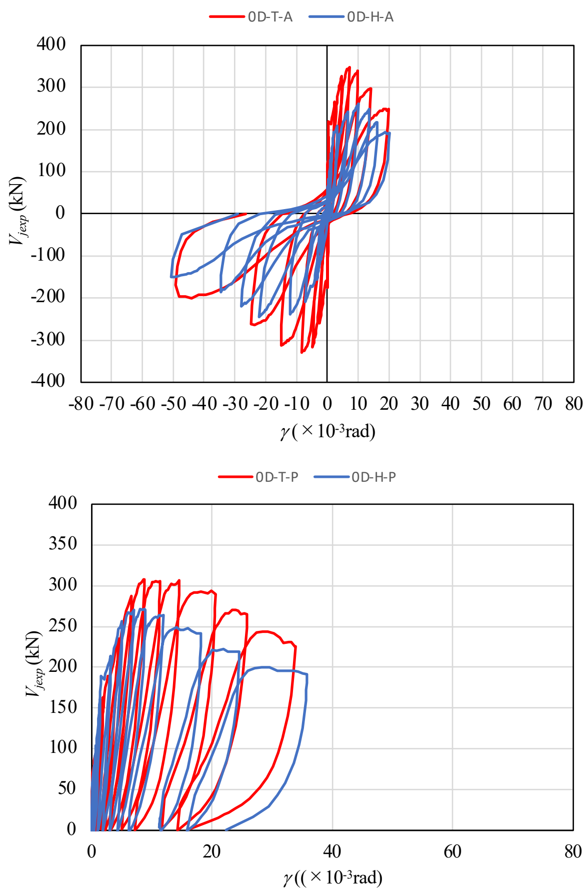

Fig. 5. Applied load–drift angle relationship

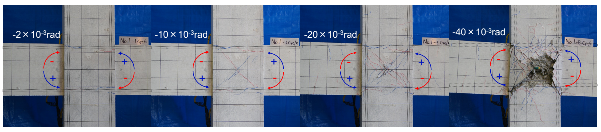

a.0D-T-A

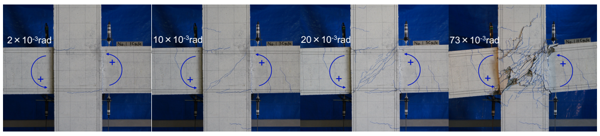

b.0D-T-P

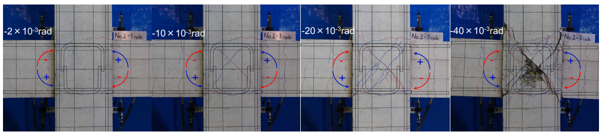

c.0D-H-A

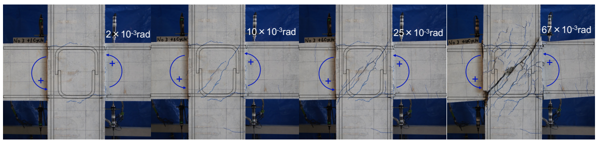

d.0D-H-P

Fig. 6. Crack patterns and failure progress

of the beams toward the bent portions of the beam main bars. This observation suggests that the compressive strut mechanism developed within the joint differs depending on the anchorage type of the beam main bars.

In all specimens, severe opening of the diagonal cracks and spalling of concrete in the panel zone cause the failure of the joint. No yielding of main bars, both in beam and column, was observed. As shown by the shear deformation angles in Fig. 5, the shear deformation of the joint accounted for approximately half of the total drift angle in all specimens. Based on these results, it is recognized that all specimens failed by shear in the panel zone.

3.2 Strains of Main Bars

Fig. 7 shows the strain distribution of the beam main bars. In specimen 0D-T-A. During positive loading (blue plots), steep strain gradients were observed in the right region of the beam main bars, indicating the development of large bond stresses near the compression edge of the column. In contrast, during negative loading (red plots), the strain gradients in the same region became relatively shallow, suggesting that only small bond stresses developed there. These observations suggest that bond deterioration occurred near the tensile edge of the column. Based on these observations, the strains plotted by void marks were estimated assuming a strain distribution simi-lar to that observed in specimen 0D-T-A. In the specimens with through-bars, tensile strain was observed in the compression region of the beam. This suggests the occurrence of a “tension shift” caused by bond deterioration of the main bars due to the propagation

● : 2×10^{-3}rad ■ : 10×10^{-3}rad ▲ : 20×10^{-3}rad
(○, □, △ : Assumed strain)

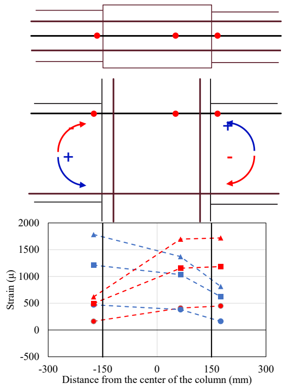

a.0D-T-A

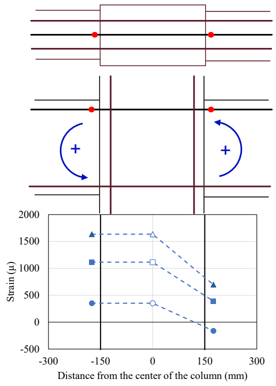

b.0D-T-P

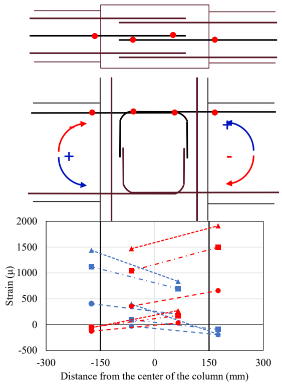

c.0D-H-A

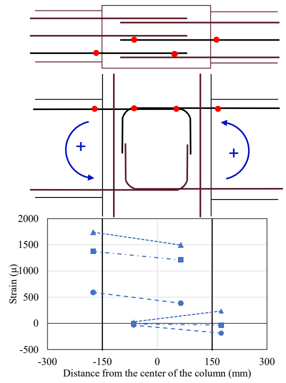

d.0D-H-P

Fig. 7. Strain distribution of main bars

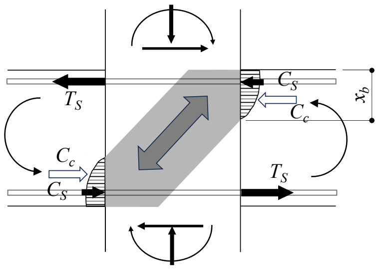

Good bond (reduced concrete compressive force)

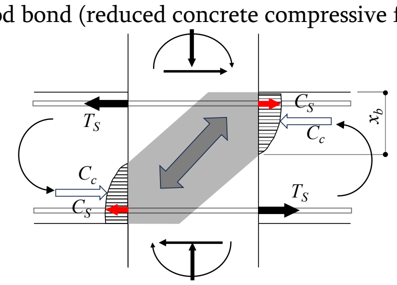

Poor bond (increased concrete compressive force)

a. 0D-T-A/P

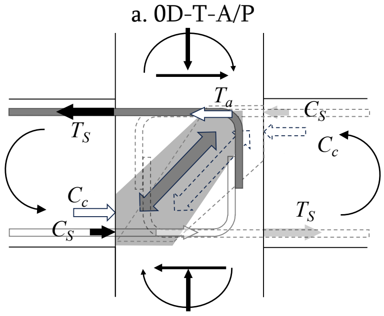

b. 0D-H-A/P

Fig. 8. Assumed concrete strut developed in the joint

of cracks within the joint. As shown in Fig. 8. a, Kusuhara et al. pointed out that the tensile conversion of compression-side beam bars enlarges the concrete compression zone. [8] Conversely, in cases such as the present experiments, where the beam main bars do not yield and the joint strength is governed by concrete compression within the joint, an increase in strut capacity enables the trans-mission of larger compressive forces, resulting in higher joint shear strength.

In contrast, in the specimens with hooked bar anchorage, the strain distribution of the beam compression-side main bars indicated little influence of tension shift. The gradients of strain in the tensile and compression bars suggest that the bond stresses developed along the horizontal portions were approximately comparable. Furthermore, the residual strain observed near the starting point of the bend implies that the anchorage force developed at the bent portion accounted for more than half of the tensile force in the beam-end tensile bars. Therefore, the stress transfer mechanism in the hooked-anchorage specimens is presumed to be as shown in Fig. 8. b, where a diagonal strut develops toward the hooked anchorage region. This observation is consistent with the occurrence of the inclined cracks propagating toward the hooked anchorage region observed in Fig. 6.

4 Discussions

Table 2 summarizes the experimental and calculated shear strengths of each specimen. The calculated shear strengths were by Eq. (2) specified in the AIJ design guidelines [1]. For the specimens with through-bars, the $V_{jexp\max}$ / V_{ju} values were approximately 1.0, indicating that the experimental joint shear strengths were reasonably evaluated by the AIJ guidelines, consistent with the observed joint shear failure. For the speci-mens with hooked bar anchorage, the AIJ guidelines overestimated the joint shear strength when D_j was taken as the column depth. However, when D_j was defined as the horizontal projected anchorage length l_{dh} (Fig.9) of the beam main bars, the $V_{jexp\max}$ / V_{ju} values approached 1.0, showing reasonable agreement with the experimentally observed joint shear failure.

$$V_{ju}=\kappa\cdot\phi\cdot F_j\cdot b_j\cdot D_j \quad (2)$$

where,

κ: coefficients depending on the geometry

ϕ : correction coefficient depending on whether or not there is a orthogonal beam

F_j : ($=\sigma_B^{0.7}$) standard value for joint shear strength

Table 2. Maximum applied load and maximum shear force in panel zone

Test specimen	Maximum beam load (kN)		Maximum shear force (kN)				
	$P_{exp\max}$	R (%)	$V_{jexp\max}$	$V_{ju(AIJ)}$ $D_j=D_c$	$V_{ju(AIJ)}$ $D_j=l_{dh}$	$V_{jexp\max}/V_{ju}$ $D_j=D_c$	$V_{jexp\max}/V_{ju}$ $D_j=l_{dh}$
0D-T-A	+43.1/ -40.5	2.0	+349/-328	327	-	1.07	-
0D-T-P	38.0	2.0	308	310	-	0.99	-
0D-H-A	+32.3/ -30.4	2.0	+261/-245	327	269	0.80/ 0.75	0.97/ 0.91
0D-H-P	33.7	2.5	272	299	247	0.91	1.10

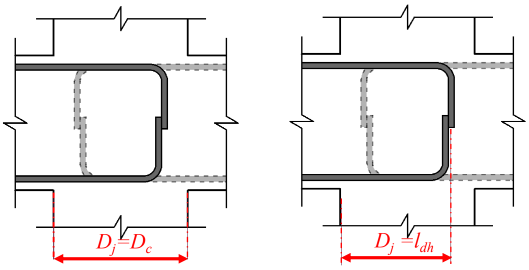

Fig. 9. Effective depth of joint

σ_B : concrete compressive strength

b_j : effective width of joint

D_j : effective depth of joint

5 Conclusions

This study experimentally investigated the influence of beam main bar anchorage type on the shear strength of interior reinforced concrete beam–column joints using cruci-form joint specimens with through-bar and hooked anchorage details. Based on the test results, the following conclusions were obtained:

1. The specimens with hooked bar anchorage exhibited lower shear strength than those with through-bars. The maximum strengths of the hooked anchorage spec-imens were approximately 11–25% lower than those of the corresponding through-bar specimens.
2. In the specimens with through-bars, typical diagonal shear cracks connecting the compression zones of the beam and column were observed, whereas the speci-mens with hooked anchorage showed inclined cracks propagating toward the hooked anchorage region. These differences indicate that the compressive strut mechanism within the joint differs depending on the anchorage type of the beam main bars.
3. In the specimens with through-bars, tensile strain developed in the compression-side of beam due to bond deterioration and tension shift within the joint. In contrast, the hooked anchorage specimens showed little influence of tension shift, and a significant portion of the tensile force was

transferred through an-chorage action at the bent portion of the bars.

4. For the specimens with through-bars, the experimental shear strengths were reason-ably evaluated by the AIJ design guidelines. For the specimens with hooked an-chorage, the AIJ guidelines overestimated the shear strength when the effective joint depth was taken as the column depth. A reasonable agreement was recog-nized when the horizontal projected anchorage length of the beam main bars is used as the effective depth of the column.

This achievement was supported by JST SPRING, Grant Number JPMJSP2124. In conducting this research, we received valuable assistance from graduates of the Hanai Laboratory at Kyushu Sangyo University, as well as invaluable advice from Professor Toshihiko Ninakawa of Kyushu University. We express sincere gratitude to them here.

References

Books

1. Architectural Institute of Japan, Design Guidelines for Earthquake Resistant Reinforced Concrete Buildings Based on Inelastic Displacement Concept, AIJ, Tokyo(1999).
2. ACI 352R-02: Recommendations for Design of Beam–Column Connections in Monolithic RC Structures (2002).
3. EN 1998-1: Eurocode 8 – Design of Structures for Earthquake Resistance, Part 1: General Rules, Seismic Actions and Rules for Buildings(2004).
4. NZS 3101: Concrete Structures Standard – Part 1: The Design of Concrete Structures, (Amendment 3) (2017).

Journal articles

5. Kazuhiro Kitayama: The State of the Art on Bond Characteristics along Bars Passing through R/C Beam-Column Joint, Concrete Journal Vol. 33, No. 5, pp. 25-33 (1995)

Proceedings

6. Kondo, S., Nishihara, H., Matsumoto, T., and Suzuki, H.: Experimental Study on Beam–Column Joints with Bent-Up Bar Anchorage, Proceedings of the Japan Concrete Institute Annual Conference, Vol.15, No.2, pp.595-600 (1993)
7. Tianwen Dong, Hanai Nobuaki: Experimental Study on Ultimate Shear Strength of Reinforced Concrete Beam-Column Joint when being Different Anchorage Type, Proceedings of the Japan Concrete Institute Annual Conference, Vol.41, No.2, pp.313–318 (2019).
8. Fumio Kusuhara, Hitoshi Shiohara: Causal relationship between joint shear force and joint failure of RC column beam joints preceded by joint failure, Proceedings of the Japan Concrete Institute, Vol.19, No.2, pp.1005-1010 (1997)